Movement and interplay of the bound state, resonance, and shadow poles of the scattering amplitude in multiphoton processes

R. M. Potvliege and Robin Shakeshaft
Physics Department, University of Southern California, Los Angeles, California 90089-0484
(Received 6 July 1988)

We examine, in a heuristic fashion, the analytic structure of the scattering amplitude for an electron interacting with an atomic potential in the presence of a radiation field. For each resonance pole of the amplitude there are infinitely many shadow poles lying on different unphysical energy sheets of the infinitely many sheeted Riemann surface. The pole having the dominant influence on the scattering amplitude is the one closest to the physical energy axis. All poles undergo significant movement when the field intensity is varied, and when a resonance pole which is dominant passes by a multiphoton ionization threshold a shadow pole usually moves closer to the physical energy axis and hence becomes the dominant pole. When this happens, an initially bound electron may jump eigenvalue curves, and in this way the electron can undergo a very large (ponderomotive) shift in its energy and still maintain the correct physical character of its wave function. The movement of resonance poles near thresholds has implications for the fate of autoionizing states and for population trapping. Consideration of threshold effects might also shed light on a puzzling result of a recent energy-shift measurement. We address the problem of how to determine, in numerical calculations, which sheet the energy eigenvalue is on so that the dominant pole can be identified. We illustrate some of our remarks by results of numerical calculations, and we also touch on the question of the completeness of a basis set in numerical calculations of resonance eigenvalues.

I. INTRODUCTION

To calculate the rate of decay of an atom in the presence of a monochromatic radiation field, one must effectively determine the locations of one or more poles of the resolvent operator for the system (atom plus field). In this paper we discuss the various classes of poles, in particular the class of "shadow" poles, which has received little attention in the multiphoton physics literature. The shadow poles, as distinguished from the "dominant" poles, normally have only a weak influence on the physical scattering amplitude. However, as the intensity or frequency of the laser is varied, the various poles move, and when a multiphoton ionization threshold is passed a pole which is a dominant one may change roles with a shadow pole; in other words, a shadow pole may become a dominant one. We present results of calculations of the pole trajectories for a model atom and show that care must be taken to correctly identify the dominant pole.

Any atomic Hamiltonian H_a may support bound states, which are stable, and resonance states, which are unstable.[1] These states are represented by regular solutions to the time-independent Schrödinger equation which satisfy (in coordinate space) an outgoing-wave boundary condition at asymptotically large distances. (The outgoing wave decays in space if the electron is bound.) To each bound state or resonance there corresponds a pole of the resolvent $R_a(E)=1/(E-H_a)$. The resolvent is multivalued in E because for each E there are two choices for the asymptotic boundary condition—outgoing *or* ingoing waves. Furthermore, the full specification of the asymptotic boundary condition requires the specification of the channel into which the atom can disintegrate if its energy exceeds the ionization threshold. Thus $R_a(E)$ must be defined on a Riemann surface consisting of 2^N energy sheets, where N is the number of channels. The *physical* energy sheet is the one whose real axis contains the physically allowed energies, that is, those energies which correspond to physically realizable wave functions. Bound-state poles of $R_a(E)$ lie on the negative real axis of the physical sheet while resonance poles lie on unphysical sheets. If a resonance pole is to have a significant physical effect, it must not lie far from the physical energy axis.

When an atom interacts with another system, for example, a radiation field, it will in general break up. Nevertheless, information on the bound states and resonances of the original atom is retained in the resolvent, $R(E)$, of the joint system; $R(E)$ has poles that are just the bound-state and resonance poles of $R_a(E)$ displaced from their original positions by the coupling. Since the joint system in general has more channels than the original atom, $R(E)$ is defined on a Riemann surface larger than that on which $R_a(E)$ is defined. Furthermore, $R(E)$ has additional poles—shadow poles—that are the shadows cast by the displaced bound-state and resonance poles of $R_a(E)$ on some of the additional unphysical sheets of the larger Riemann surface. If the interaction between the atom and the second system is very weak, a displaced bound-state or resonance pole of $R_a(E)$ will lie closer to the physical energy axis than the shadow poles which it casts; in this circumstance it is the displaced poles of $R_a(E)$ that are the *dominant* poles.

Shadow poles were first discussed in the context of elementary particle physics, by Eden and Taylor[2] in particu-

lar, but also by many others.[3] Experimental evidence of the existence of these poles has been seen in observations of resonances in high-energy physics[4] and, more recently, in nuclear physics.[5] Shadow poles have also been discussed in the context of atomic physics, as, for example, in the interpretation of the threshold behavior of the cross section for excitation of the 2^3S state of He by electron impact,[6] and in the analysis of processes such as dissociative attachment, and collisional electronic excitation of molecules.[7] However, aside from the study by Ostrovskii[8] of an electron moving in a one-dimensional zero-range (δ function) potential which is harmonic in time, there seems to have been little discussion of shadow poles in the context of multiphoton processes. Yet it is in the domain of multiphoton processes that shadow poles may perhaps be of greatest interest. This is because the strength of the coupling between an atom and a laser field can be varied at will, by varying either the intensity or the frequency of the laser. The poles of $R(E)$ move around on the Riemann surface as the coupling strength varies; that substantial movement can occur may be appreciated on recalling that the ionization energy of an atom is increased in the presence of an intense low-frequency laser field by roughly the ponderomotive energy shift, which is proportional to the laser intensity and routinely exceeds 15 eV in current multiphoton ionization experiments[9] utilizing a laser of frequency 1.2 eV. Thus a bound-state pole of $R_a(E)$ may be displaced, by the field, down the (underside of the) negative-energy axis and past one or more channel thresholds. As we see below, and as noted earlier by Ostrovskii,[8] when a threshold is passed one of the shadow poles moves closer to the physical energy axis than the pole which is dominant before the threshold is passed, and it consequently becomes the dominant pole. Consideration of threshold effects might reveal an explanation for the puzzling result of a recent energy-shift measurement.[10]

Resonance poles of $R_a(E)$ also undergo large shifts in the presence of an intense laser field. The question naturally arises as to what happens when, say, an autoionizing state shifts below the ionization threshold (of the appropriate channel). There is a popular misconception that this autoionizing state becomes bound. In fact, as we see below, the dominant pole moves further away from the physical energy axis and ceases to be physically significant. Threshold effects can also have implications for the phenomenon of population trapping.

In Sec. II we give a heuristic (mathematically nonrigorous) analysis of the analytic structure of the scattering amplitude for an electron interacting with an atomic potential in the presence of a monochromatic, spatially homogeneous, radiation field. We restrict our discussion for the most part to atomic potentials which decrease at large distances faster than the Coulomb potential so as to avoid the complications arising from an accumulation of bound states at each channel threshold. We focus on the simplest trajectories; the poles do not need to follow complicated—and unlikely—trajectories in order to arrive at interesting physical situations. In Sec. III we present the results of calculations for a model one-electron "atom" whose atomic potential is a sum of Yukawa potentials. We plot the trajectories, versus the laser intensity, of a dominant pole and some of its associated shadow poles and we demonstrate the typical behavior of these poles. Our calculation, which involves the expansion of the electron wave function on a finite basis set, cannot reveal all of the shadow poles. This is because our basis (even when enlarged indefinitely) is incomplete, not in the usual sense (of completeness in a Hilbert space of normalizable functions), but in the sense that it cannot represent both ingoing and outgoing waves; this is discussed more fully in Sec. III. We comment on how this difficulty can be alleviated.

II. GENERAL ANALYSIS

A. Time-independent wave equation

For simplicity we consider an atomic system that has only one electron. We can express the interaction of this electron with the spatially homogeneous radiation field as

$$V(t)=V_+e^{-i\omega t}+V_-e^{i\omega t}\ , \tag{2.1}$$

where ω is the field frequency and where V_+ and $V_-=V_+^\dagger$ are time independent. We adopt the velocity gauge, in which case $V_+=-(e/2\mu c)(\mathbf{A}_0\cdot\mathbf{p})$, where e, μ, and $\mathbf{p}$ are the charge, mass, and canonical momentum (operator) of the electron and where $\mathbf{A}_0$ is the amplitude of the vector potential $\mathbf{A}(t)=\mathrm{Re}(\mathbf{A}_0e^{-i\omega t})$. Note that we have omitted the term $e^2\mathbf{A}(t)^2/(2\mu c^2)$ from $V(t)$; this term is spatially-independent and can be removed by a simple gauge transformation. Its removal cancels the upward pondermotive energy shift of the continuum by shifting the energy spectrum downwards by the amount

$$\begin{aligned}P&=\frac{\omega}{2\pi}\int_0^{2\pi/\omega}dt\frac{e^2\mathbf{A}^2(t)}{2\mu c^2}\\&=(e^2/4\mu c^2)\,\mathbf{A}_0\cdot\mathbf{A}_0^*\ .\end{aligned} \tag{2.2}$$

Throughout this paper we keep ω fixed but allow the intensity $\omega^2|\mathbf{A}_0|^2/8\pi c$ to vary.

To pass to the time-independent treatment we make the Floquet ansatz[11] for $|\Psi(t)\rangle$, the electron wave vector:

$$|\Psi(t)\rangle=e^{-iEt/\hbar}|\Phi(t)\rangle\ , \tag{2.3}$$

where E is the electron quasienergy and $|\Phi(t)\rangle$ is periodic in t with period $2\pi/\omega$. Substituting (2.3) into the Schrödinger equation

$$[i\hbar(d/dt)-H_a-V(t)]|\Psi(t)\rangle=0\ , \tag{2.4}$$

and using Eq. (2.1) together with the harmonic expansion

$$|\Phi(t)\rangle=\sum_n e^{-in\omega t}|\phi_n\rangle\ , \tag{2.5}$$

we obtain the following coupled equations for the time-independent harmonic components $|\phi_n\rangle$:

$$(E+n\hbar\omega-H_a)|\phi_n\rangle=V_+|\phi_{n-1}\rangle+V_-|\phi_{n+1}\rangle\ . \tag{2.6}$$

B. Asymptotic boundary condition

At asymptotically large distances the electron is free of the atomic potential. However, in a time-independent treatment we cannot switch the field on or off and therefore the field persists even when the electron is infinitely far from the atomic potential. This does not pose any serious difficulty since the wave vectors of a *free* electron in the absence and in the presence of the field are related by the unitary operator

$$O(t)=e^{-i\alpha(t)\cdot\mathbf{p}/\hbar}, \tag{2.7a}$$

$$\alpha(t)=-(e/\mu c)\int^t dt'\ \mathbf{A}(t') . \tag{2.7b}$$

Thus at asymptotically large distances $[O(t)]^{-1}\,|\,\Psi(t)\rangle$ represents a free electron in the absence of the field. The canonical momentum operator $\mathbf{p}$ commutes with $V(t)$ and therefore the canonical momentum of the electron, which in the presence of the field is the mean momentum averaged over one cycle, would be unaffected by switching the field on or off when the electron is asymptotically far away. Indeed, the states represented by $|\,\Phi(t)\rangle$ and $[O(t)]^{-1}\,|\,\Phi(t)\rangle$ have the same momentum distributions. Hence if the electron is incident from infinity along the direction of the unit vector $\hat{\mathbf{u}}$, with mean momentum $\hbar k_0\hat{\mathbf{u}}$, and if it absorbs m photons so as to emerge from the scattering region with mean momentum $\hbar k_m\hat{\mathbf{x}}$, we have, summing over m,

$$\langle\mathbf{x}\,|\,[O(t)]^{-1}\,|\,\Phi(t)\rangle \rightarrow Ce^{ik_0\hat{\mathbf{u}}\cdot\mathbf{x}}+\sum_m e^{-im\omega t}f_m(E,\hat{\mathbf{x}})e^{ik_m r}/r , \tag{2.8}$$

where C is the amplitude of the incident wave, which is specified in advance, and where $r=|\,\mathbf{x}\,|\sim\infty$, $\hat{\mathbf{x}}=\mathbf{x}/r$, and

$$k_m=[(2\mu/\hbar^2)(E+m\hbar\omega)]^{1/2} . \tag{2.9}$$

[If the potential has a Coulomb tail, the logarithmic distortion must be included in the phases on the right-hand side of Eq. (2.8).] From Eqs. (2.7) and (2.8) we obtain

$$\langle\mathbf{x}\,|\,\Phi(t)\rangle \rightarrow Ce^{-ik_0\hat{\mathbf{u}}\cdot\alpha(t)}e^{ik_0\hat{\mathbf{u}}\cdot\mathbf{x}} + \sum_m e^{-im\omega t-ik_m\hat{\mathbf{x}}\cdot\alpha(t)}f_m(E,\hat{\mathbf{x}})e^{ik_m r}/r . \tag{2.10}$$

Since the Schrödinger equation is linear and homogeneous, the amplitude $f_m(E,\hat{\mathbf{x}})$ for absorption of m real photons is proportional to C. Hence if we let C approach zero, $f_m(E,\hat{\mathbf{x}})$ vanishes (there can be no scattered wave if there is no incident wave) except for those values of E for which, when C is nonzero, $f_m(E,\hat{\mathbf{x}})$ has a pole. At values of E for which $f_m(E,\hat{\mathbf{x}})$ has a pole, the wave function can satisfy a pure outgoing-wave asymptotic boundary condition, corresponding to a bound state or resonance. Let us transform the summation index on the right-hand side of Eq. (2.8) or (2.10) from m to $m+l$, and factor $\exp(-il\omega t)$ out of the sum. We cannot interpret $f_{m+l}(E,\hat{\mathbf{x}})$ as the m-photon absorption amplitude for an electron incident with energy $E+l\hbar\omega$ because the first term on the right-hand side of (2.8) or (2.10) represents an electron incident with energy E. However, if $f_m(E,\hat{\mathbf{x}})$ has a pole at $E=E_p$, we can put $C=0$, in which case the asymptotic boundary condition is identical for $E=E_p$ and $E=E_p+l\hbar\omega$; it then follows that $f_{m+l}(E_p,\hat{\mathbf{x}})$ is proportional to $f_m(E_p+l\hbar\omega,\hat{\mathbf{x}})$. In other words if $f_m(E,\hat{\mathbf{x}})$ has a pole at $E=E_p$, $f_{m+l}(E,\hat{\mathbf{x}})$ must have a pole at $E=E_p-l\hbar\omega$. (However, the pole at E_p does not necessarily lie on the same sheet as the pole at $E_p-l\hbar\omega$.)

At nonsingular values of E the normalization of $|\,\Phi(t)\rangle$, and therefore $f_m(E,\hat{\mathbf{x}})$, are fixed by C, the amplitude of the incident wave. At singular values of E, the normalization of $|\,\Phi(t)\rangle$ may be fixed by the physically appropriate boundary condition on the "incident" wave. If the electron is initially bound, the incident wave is represented by the normalized bound-state wave function immediately after the field has been turned on, and the normalization of $|\,\Phi(t)\rangle$ is fixed by the condition that the probability for finding the electron in the "incident" wave diminishes in time at the decay rate of the atom.[12] The properly normalized $f_m(E,\hat{\mathbf{x}})$ are finite at the singular values of E [the singular $f_m(E,\hat{\mathbf{x}})$ are renormalized through multiplication by a factor proportional to $E-E_p$]. Furthermore, since, at the singular values of E, both the asymptotic boundary condition and the normalization condition are the same whether $|\,\Phi(t)\rangle$ is defined in terms of $f_{m+l}(E,\hat{\mathbf{x}})$ or $f_m(E+l\hbar\omega,\hat{\mathbf{x}})$, we have

$$f_{m+l}(E_p,\hat{\mathbf{x}})=f_m(E_p+l\hbar\omega,\hat{\mathbf{x}})$$

under the proper renormalization.

The asymptotic boundary condition satisfied by the harmonic components is given, from Eqs. (2.5) and (2.10), as

$$\langle\mathbf{x}\,|\,\phi_n\rangle\rightarrow C_n e^{ik_0\hat{\mathbf{u}}\cdot\mathbf{x}}+\sum_m f_{mn}(E,\hat{\mathbf{x}})e^{ik_m r}/r , \tag{2.11a}$$

where, writing $\mathbf{k}_m\cdot\boldsymbol{\alpha}(t)=\rho_m\sin(\omega t-\chi_m)$, where ρ_m and χ_m are both real and depend on $\mathbf{k}_m=k_m\hat{\mathbf{x}}$, writing $k_0\hat{\mathbf{u}}\cdot\boldsymbol{\alpha}(t)=\rho\sin(\omega t-\chi)$, and using the integral representation

$$J_n(z)=\frac{1}{2\pi}\int_0^{2\pi}d\tau\, e^{in\tau-iz\sin\tau}$$

for the Bessel function, we have

$$C_n=e^{in\chi}J_n(\rho)C , \tag{2.11b}$$

$$f_{mn}(E,\hat{\mathbf{x}})=e^{i(n-m)\chi_m}J_{n-m}(\rho_m)f_m(E,\hat{\mathbf{x}}) . \tag{2.11c}$$

A harmonic component $|\,\phi_n\rangle$ represents the electron after it has absorbed a total of n photons, both real and virtual, and $f_{mn}(E,\hat{\mathbf{x}})$ is the amplitude that the electron has absorbed m *real* photons when it absorbs a total of n photons. The net amplitude $f_m(E,\hat{\mathbf{x}})$ for absorbing m real photons is a coherent sum over all possible virtual absorptions. In the zero-field limit we have $f_{mn}(E,\hat{\mathbf{x}})=f_m(E,\hat{\mathbf{x}})\delta_{mn}$. From Eq. (2.11c) we see that if $f_m(E,\hat{\mathbf{x}})$ has a pole at $E=E_p$, so does $f_{mn}(E,\hat{\mathbf{x}})$; the converse is also true. Furthermore, provided that the field is on, a pole of $f_m(E,\hat{\mathbf{x}})$ must give rise to a pole of $f_l(E,\hat{\mathbf{x}})$ at the same location on the same sheet, for all l, since all

channels are coupled together, as illustrated by the coupled equations (2.6) for the harmonic components. In summary, if $f_m(E,\hat{\mathbf{x}})$ has a pole at $E=E_p$, which may move but does not disappear in the zero-field limit, we conclude that when the field is on $f_l(E,\hat{\mathbf{x}})$ and $f_{ln}(E,\hat{\mathbf{x}})$ have poles at $E=E_p+l'\hbar\omega$ for all (integer) l and l'; in the zero-field limit the residues of these poles vanish unless $l'=m-l$. A pole of $f_m(E,\hat{\mathbf{x}})$ at $E=E_p$ corresponds to an outgoing-wave solution of Eqs (2.6) with complex eigenvalue E_p.[13]

It is important to note that the asymptotic boundary conditions stated above apply only in the velocity gauge; they do not apply in the length gauge since in the latter gauge the canonical momentum is the instantaneous momentum, not the mean momentum. [Moreover, in the length gauge $V(t)$ diverges in position space for $r\sim\infty$. Of course, in the velocity gauge, $V(t)$ diverges in momentum space for $p\sim\infty$, but it does not diverge as fast as $p^2/2\mu$.] This has important consequences[14] for the formulation of a time-independent treatment of multiphoton processes.

In the Appendix we derive two different expressions for the m-photon absorption rate $f_m(E,\hat{\mathbf{x}})$, one in terms of matrix elements of the coupling V_+ of the electron to the field, the other in terms of matrix elements of the coupling of the electron to the atomic potential.

C. Riemann surface and the optical theorem

We must now specify the branch of the square root of Eq. (2.9). On the *physical* energy sheet we have $0\le\arg(k_m)<\pi$ for all m. We draw a series of overlapping branch cuts along the real energy axis, with the mth branch cut originating at the threshold $E=-m\hbar\omega$ (the threshold of channel m) and extending to ∞. Unphysical energy sheets are reached from the physical sheet by paths crossing some of the branch cuts. On an unphysical sheet we have $-\pi\le\arg(k_m)<0$ for at least one value of m. The physically allowed values of E are those that lie on the real axis on the physical energy sheet. For the remainder of this paragraph we assume that E is physically allowed. If $N_0(E)$ is the smallest integer for which $E+N_0(E)\hbar\omega\ge 0$, we have that k_m is real and nonnegative if $m\ge N_0(E)$ and that k_m is positive imaginary if $m<N_0(E)$; the terms in the sum on the right-hand side of Eq. (2.10) represent outgoing scattered waves if $m\ge N_0(E)$ (open channels) and outgoing decaying waves if $m<N_0(E)$ (closed channels). The total probability current radiated to infinity is, from Eq. (2.10),

$$j_{\rm rad}=\sum_{m\ge N_0(E)}\frac{\hbar k_m}{\mu}\int d\hat{\mathbf{x}}\,|f_m(E,\hat{\mathbf{x}})|^2\,, \tag{2.12}$$

where cross terms have been neglected since they vanish when averaged over a macroscopically small volume. If E is positive, k_0 is real and positive and the first term on the right-hand side of Eq. (2.10) represents a wave of specified amplitude C incident from infinity. The probability current lost from the incident beam is given as the interference between the incident wave and the radiated wave, integrated over a surface perpendicular to $\hat{\mathbf{u}}$ which subtends a very small solid angle that includes $\hat{\mathbf{u}}$. The loss is

$$j_{\rm loss}=\frac{4\pi\hbar}{\mu}{\rm Im}[C^*f_0(E,r\hat{\mathbf{u}})]\,, \tag{2.13}$$

where terms involving $f_m(E,r\hat{\mathbf{u}})$ with $m\neq 0$ have been neglected since they average to zero over a macroscopically small volume. Since E is physically allowed, current must be conserved and we have the optical theorem $j_{\rm rad}=j_{\rm loss}$.

The optical theorem, which applies only for physically allowed values of E, immediately tells us that $f_m(E,\hat{\mathbf{x}})$, for $m\ge N_0(E)$, cannot have a pole at a physically allowed positive value of E, since otherwise $j_{\rm rad}$ would possess a pole whose order would be the square of the order of the pole contained in $j_{\rm loss}$, if indeed $j_{\rm loss}$ contained a pole at all. Furthermore, except in the zero-field limit, $f_m(E,\hat{\mathbf{x}})$ cannot have a pole at a physically allowed positive value of E even if $m<N_0(E)$. This follows because, with the field on, a pole of $f_m(E,\hat{\mathbf{x}})$ gives rise to a pole of $f_l(E,\hat{\mathbf{x}})$ at the same location on the same sheet, for all l, and in particular $l\ge N_0(E)$, since all channels are coupled together. Of course, there would be no objection to $f_l(E)$ having a pole on the positive physical energy axis when $l\ge N_0(E)$ if the pole were to have a vanishing residue; this is relevant to population trapping, discussed below. We also see from the optical theorem that, except in the zero-field limit, there are no *negative* physically allowed values of E for which the asymptotic boundary condition (2.10) can be satisfied, since for such values k_0 would be imaginary and the first term on the right-hand side of Eq. (2.10) would be unphysical, unless $C=0$, in which case $f_m(E,\hat{\mathbf{x}})$ would have a pole on the negative physical energy axis, at $E=E_b-m\hbar\omega$ say; but $f_m(E,\hat{\mathbf{x}})$ would also have a pole at $E=E_b+l\hbar\omega$, all l, and we could choose l sufficiently positive that this pole lies on the positive physical energy axis, in contradiction with the above. Of course, in the zero-field limit negative values of E are physically allowed, namely, those discrete values corresponding to the bound states. [In the zero-field limit the residue of the pole of $f_m(E,\hat{\mathbf{x}})$ at $E=E_b+l\hbar\omega$ vanishes if $l\neq -m$ because the interchannel coupling vanishes.] When the field is turned on the bound-state poles shift off the real axis. Furthermore, they must shift onto an unphysical sheet, and hence become resonance poles; were they to remain on the physical sheet we would have ${\rm Im}(k_m)>0$, all m, and the wave function would decay at large distances and would not, therefore, represent an electron escaping to infinity. Therefore the trajectories of the bound-state poles must cross the real energy axis, along which the branch cuts lie, to an unphysical sheet where the energy has a negative imaginary part, $-\Gamma/2$ say. (See Fig. 1.) The decay rate of the atom is $\Gamma/\hbar$, as is evident from Eq. (2.3) which shows $|\Psi(t)\rangle$ decreasing exponentially with time as $\exp(-\Gamma t/2)$. Provided that the bound-state poles do not move far from the real axis, that is, provided that the imaginary part of E is small compared to the real part, we can recover the optical theorem by neglecting the imaginary part of E in the evaluation of $j_{\rm rad}$ and by equating $j_{\rm loss}$ with $\Gamma/\hbar$, the to-

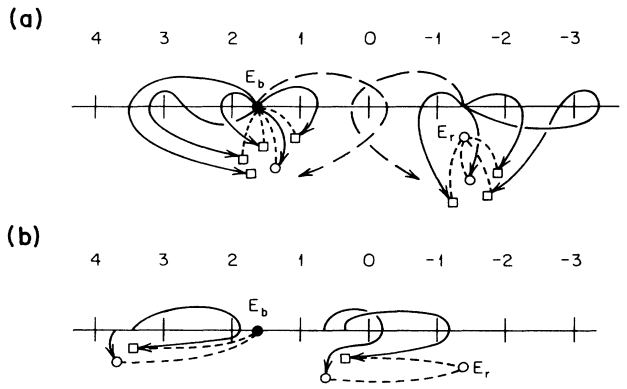

FIG. 1. Some possible trajectories (short dashed lines) of poles of $f_0(E,\hat{\mathbf{x}})$ in the complex E plane vs intensity. In the zero-field limit $f_0(E,\hat{\mathbf{x}})$ has a bound-state pole (solid circle) at E_b and a resonance pole (open circle) at E_r. The straight horizontal line is the real energy axis, and the short vertical lines mark the channel thresholds, which are numbered. When the field is turned on the bound-state pole moves off the real axis and becomes a resonance pole; the pole which is a resonance pole in the zero-field limit also moves. The shadow poles (open squares) move to different positions. The solid lines are possible paths from the physical energy axis to the poles. The dominant pole (open circle) is closer to the physical energy axis than the shadow poles, and can be reached by a path which does not encircle a threshold. The long-dashed lines in (a) are example of paths from the physical energy axis to unphysical sheets on which there are no shadow poles. In (b) the dominant pole (open circle) has interchanged roles with a shadow pole; the open square was the dominant pole along the initial portion of the trajectory before it passed to the left of the threshold of channel 2.

tal rate of decay of the bound state. The degree to which this modified optical theorem is satisfied is, in fact, a measure of the applicability of the Floquet ansatz to ionization processes.[15]

D. Shadow poles

In Fig. 1 we show the hypothetical behavior of a resonance pole which develops from a bound-state pole as the intensity of the field is varied. Suppose for the moment that the field is off. In this limit $f_l(E,\hat{\mathbf{x}})$ has a bound-state pole on the physical sheet at $E=E_b-l\hbar\omega$. We focus on the pole of $f_0(E,\hat{\mathbf{x}})$ at E_b. (Since E_b lies between the thresholds of channels 1 and 2, the atom must absorb at least two photons to ionize, in the weak-field limit.) Not only does $f_0(E,\hat{\mathbf{x}})$ have a pole on the physical sheet, but this amplitude must also have a pole, at exactly the same location E_b, on the unphysical sheet reached from the physical sheet by a path which encircles once the ionization threshold of channel 1, crossing the branch cut emanating from the threshold of channel 1 [so that $\arg(k_1)$ changes from $\pi/2$ to $-\pi/2$]. This follows (we borrow the argument of Eden and Taylor[2]) because, in the zero-field limit, channel 0 is uncoupled to other channels and therefore $f_0(E,\hat{\mathbf{x}})$ should not have a branch point singularity at the thresholds of channels n, $n\neq 0$. Consequently, $f_0(E,\hat{\mathbf{x}})$ should return to its initial value along a path which starts at E_b on the physical sheet and ends at E_b on the unphysical sheet reached by encircling the threshold of channel 1. Using similar reasoning, $f_0(E,\hat{\mathbf{x}})$ should also have a pole at E_b on the unphysical sheet reached by encircling once the threshold of channel 2 [so that $\arg(k_2)$ changes from 0 to $-\pi$]; and so on *ad infinitum*. Thus in the zero-field limit $f_0(E,\hat{\mathbf{x}})$ has a bound-state pole at E_b on the physical sheet, and it has a "shadow" pole at the same location on each unphysical sheet on which $\arg(k_0)=\pi/2$ (rather than $-\pi/2$). However, once the field is turned on, channel 0 becomes coupled to all other channels and $f_0(E,\hat{\mathbf{x}})$ acquires branch point singularities at all channel thresholds. Consequently, when the field is turned on and the poles of $f_0(E,\mathbf{x})$, which are situated at the same point E_b in the zero-field limit, move off the real axis, they do not need to move to the same locations on the various sheets. Hence $f_0(E,\hat{\mathbf{x}})$, and indeed $f_m(E,\hat{\mathbf{x}})$, have infinitely many poles displaced slightly from each other and from the zero-field bound-state pole at E_b. Each of these poles is on a different unphysical sheet. However, the pole which moves off the physical energy axis remains, at least in the weak-field limit, close to this axis—this is the dominant pole; the other poles—the shadow poles—are far from the physical energy axis. Since $f_l(E,\hat{\mathbf{x}})$ has a pole at $E=E_b-l\hbar\omega$ in the zero-field limit, and since a pole of $f_l(E,\hat{\mathbf{x}})$ is also a pole of $f_m(E,\hat{\mathbf{x}})$ when the field is on, we can generalize our conclusion and say that $f_m(E,\hat{\mathbf{x}})$, where m is an arbitrary integer, possesses infinitely many clusters of poles; each cluster is centered (at least in the weak-field limit) near a different point $E=E_b-l\hbar\omega$ and contains one dominant pole close to the physical energy axis and infinitely many shadow poles. The partial rate for ionization into the mth channel, via the absorption of m photons, is, aside from a normalization factor, $(\hbar k_m/\mu)\,|f_m(E,\hat{\mathbf{x}})|^2$, where $f_m(E,\hat{\mathbf{x}})$ must be evaluated at the real *physical* energy E that is closest to the position of the dominant resonance pole which develops from the zero-field bound-state pole at E_b (see the Appendix).

The same argument can be applied to poles of $f_m(E,\hat{\mathbf{x}})$ which arises from resonances, rather than bound states, in the zero-field limit. (See Fig. 1.) If, in the zero-field limit, $f_l(E,\hat{\mathbf{x}})$ has a resonance pole at $E=E_r-l\hbar\omega$, reached from the physical sheet by a path crossing the real axis to the right of the threshold of channel l, there are shadow poles at $E=E_r-l\hbar\omega$ on all other unphysical sheets on which $\arg(k_l)<0$, and when the field is on these (displaced) poles are also poles of $f_m(E,\hat{\mathbf{x}})$ even if $m\neq l$.

E. Conjugate poles

If there is a pole, at $E=E_p$ say, in the lower half E plane, there is also a "conjugate" pole at E_p^* in the upper half E plane on the same unphysical sheet. This follows by taking the complex conjugate of Eq. (2.4), noting that H_a is real, and transforming from t to $-t+\alpha$, where α is a constant chosen so that $\bar{V}(t)=V^*(-t+\alpha)$, where $\bar{V}(t)$ is obtained from $V(t)$ by changing $V_\pm$ to $V_\pm^\dagger$, and it corresponds to reversing the sense of field polarization (the eigenvalue spectrum is unchanged); if K denotes the operation of complex conjugation, $K|\Psi(-t+\alpha)\rangle$ is a solution of Eq. (2.4), equal to (to within a constant phase

factor) $\exp(-iE^*t/\hbar)K|\Phi(-t+\alpha)\rangle$. Hence if E_p is an eigenvalue, so is E_p^*. A conjugate pole at E_p^* is always further from the physical energy axis than the pole at E_p (in the lower half E plane) since the conjugate pole can only be reached from the physical energy axis by an additional circuit around a threshold. Conjugate poles are therefore of little physical significance, as can also be seen from the fact that an eigenfunction whose energy eigenvalue has a positive imaginary part *increases* in time. We restrict our attention in this paper to poles lying in the lower half E plane. The wave number k_m therefore lies either in the upper left or lower right quadrant of the k plane. (For the conjugate pole, k_m lies either in the upper right or lower left quadrant.) It could happen, however, that the trajectory of a pole crosses the real energy axis one or more times.

F. Interchange of dominant and shadow poles

Normally the real component of the shift in the energy of a bound-state (or resonance) pole is substantially larger than the imaginary component. If the field is of low frequency, and not too strong, the decay rate of the atom, $\Gamma/\hbar$, will be small while the ponderomotive energy shift P [of Eq. (2.2)] will, if the field is not too weak, be large. In this case, shown in Fig. 1(b), a bound-state pole will slide the distance P down the real axis past one or more thresholds as the field is turned on. (The number of photons which the atom must absorb to ionize therefore increases.[8,16]) This pole must actually slide down the *underside* of the real axis because Γ, while small, is nevertheless finite. Therefore the pole moves onto an unphysical sheet, becoming a resonance pole, and [referring to Fig. 1(b)] once it passes to the left of the threshold of channel 2 it starts to more further away from the physical energy axis because it can only be reached from the physical sheet by a path which crosses the real axis between the thresholds of channels 2 and 1. The shadow poles also shift down the underside of the real axis (along trajectories that are similar to but not the same as each other). When the pole which is dominant on the right of a threshold passes to the left, it is likely that the shadow pole which can be reached from the physical sheet by a path passing just to the left of this threshold will move closer to the physical energy axis than the other pole. This shadow pole will therefore become the dominant pole. If the new dominant pole passes to the left of another threshold it will interchange roles with still another shadow pole, and so on. This is illustrated in Fig. 1(b); the shadow pole which is reached from the physical sheet by a path which crosses the real axis between the thresholds of channels 3 and 4 becomes the dominant pole when the threshold of channel 3 is passed.

We must distinguish between a continuous "adiabatic" trajectory followed in the E plane by a given pole, and the "diabatic" trajectory which passes through whichever pole is closest to the physical energy axis at each value of the intensity. The diabatic trajectory may pass from one unphysical sheet to another, and is the path on which the dominant pole lies at each intensity; the dominant pole need not be the same pole at all intensities. Consider a pole which is dominant just before it passes to the left of the threshold of channel m, but which interchanges roles with a shadow pole when this threshold is passed. The wave number k_m of the pole which is dominant before the threshold is passed swings through an angle $\pi/2$, from an angle slightly less than zero (we assume Γ is small) to an angle slightly greater than $-\pi/2$. In contrast, if we consider the shadow pole which becomes the dominant pole, k_m swings again through an angle $\sim\pi/2$, but from an angle slightly less that π to an angle slightly greater that $\pi/2$. In the first case $\exp(ik_m r)$ changes from a weakly exploding outgoing wave to a strongly exploding one, while in the second case $\exp(ik_m r)$ changes from a weakly damped ingoing wave to a strongly damped one. Since channel m changes from an open channel to a closed one, the component of the electron wave function in the mth channel should change from a wave which is outgoing at large distances to one which is decaying. The electron must therefore follow the diabatic curve, and hence jump the gap between the adiabatic curves at the "crossing" point where these curves almost touch. The gap is of order Γ. As long as this distance is small compared to $\hbar/\Delta t$, where Δt is the characteristic time (which depends on the rate of change of intensity) for the poles to move through the crossing point, the electron can jump the gap. (If $\Gamma \gtrsim \hbar/\Delta t$ the atom ionizes before the threshold is passed.) Thus, in the vicinity of a threshold, the complete electron wave function is a superposition of *two* Floquet eigenfunctions whose eigenvalues follow one or the other of the adiabatic curves, and in principle the time-dependent coefficients for the superposition must be determined from Eq. (2.4). (This is similar[17] to the situation where the laser frequency is on resonance with the transition frequency between two bound states; in that case two poles almost coalesce on the *same* unphysical sheet, and the adiabatic curves lie on the *same* sheet, meeting at a "crossing" point which corresponds to a transition resonance rather than a threshold.) Note that the variation of the amplitude $f_m(E,\hat{\mathbf{x}})$ as a threshold is passed is rapid if the amplitude is evaluated along the adiabatic curve but slow if this amplitude is evaluated along the diabatic curve. Note also that in the neighborhood of a threshold the distinction "dominant" pole loses its meaning.

In the ultralow-frequency limit where the field becomes a static electric field of finite amplitude $\omega\mathbf{A}_0/c$, the ponderomotive shift P becomes infinite. Clearly, the energy of a bound electron does not shift by this amount. In fact, in this limit, the lifetime, $\hbar/\Gamma$, of the atomic system is smaller than the cycle time, $2\pi/\omega$, so that it makes no sense to speak of an energy shift, which is meaningful only when averaged over the cycle time. In the ultralow-frequency limit the characteristic distance Γ between two adiabatic curves at a threshold crossing point is larger than the distance $\hbar\omega$ between thresholds, and therefore crossing points merge. Hence there is no well-defined diabatic curve along which the electron can follow a smooth path.

Consider now a pole which is a resonance pole of $f_m(E,\hat{\mathbf{x}})$ in the zero-field limit, at $E_r - m\hbar\omega$ say, and which lies to the right of channel $m-p$, $p \geq 0$, and can be reached from the physical energy axis by a path passing

vertically downwards from this axis between the thresholds of channels $m-p$ and $m-p-1$. This pole is the dominant pole in the weak-field limit. However, if this pole shifts to the left as the intensity increases, it might interchange roles with a shadow pole as it shifts to the left of the threshold of channel $m-p$ if $p \geq 1$. This is because the shadow pole reached from the physical sheet by a path crossing the real axis between the thresholds of channels $m-p+1$ and $m-p$ might move closer to the physical energy axis than the resonance pole. This shadow pole would then become the dominant pole, but it might interchange roles with another shadow pole when it passes to the left of the threshold of channel $m-p+1$, if $p \geq 2$, and so on until the threshold of channel m is passed. However, once this last threshold is passed there is unlikely to be any further interchange between a shadow pole and the dominant pole. This is because the poles of $f_m(E,\hat{\mathbf{x}})$ which are born from a resonance pole, rather than a bound-state pole, of $f_m(E,\hat{\mathbf{x}})$, can only be reached from the physical energy axis by paths which cross the real axis (an odd number of times) to the *right* of the threshold of channel m.[18] Consequently, when the dominant pole moves further to the left of the threshold of channel m it actually moves further from the physical energy axis and ceases to be physically significant. This justifies our earlier remark that an autoionizing level which is shifted far below the ionization threshold will cease to be physically significant. Were an electron to be "bound" in an autoionizing state (possibly a long-lived state in the absence of the field) and were the resonance pole of $f_m(E,\hat{\mathbf{x}})$ which corresponds to this state in the zero-field limit to move below the threshold of channel m, the electron would be liberated before this threshold were reached.

It is appropriate here to mention a recent calculation[19] of the amplitude for an electron to scatter from a model potential in the presence of a laser field. It was observed in Ref. 19 that when interchannel coupling is neglected, $f_0(E,\hat{\mathbf{x}})$ acquires new bound-state poles as the laser intensity increases. These new bound-state poles presumably arise from resonance poles shifting down underneath the positive real axis, *through* the threshold of channel 0, and onto the negative physical energy axis. Such behavior is an artifact of the neglect of interchannel coupling. A dominant pole which develops from a resonance pole of $f_m(E,\hat{x})$ in the zero-field limit will not normally pass *through* the threshold of channel m; rather, this pole will pass *beneath* the threshold, and will move further from the physical energy axis as it shifts further downwards.[18]

G. Population trapping

Suppose that in the zero-field limit $f_0(E,\hat{\mathbf{x}})$ has a bound-state pole at $E=E_b$ and a resonance pole not far off the physical energy axis at $E=E_r$, and suppose also that $\mathrm{Re}(E_r)$ differs from E_b by nearly $p\hbar\omega$ (with p an integer). In the weak-field limit $f_0(E,\hat{\mathbf{x}})$ acquires a pole at $E=E_b+m\hbar\omega$ (almost) on the physical energy axis and since this pole is close to the resonance pole which appears at $E_r+(m-p)\hbar\omega$ the two poles will interact strongly and repel each other. As the laser intensity is turned up, the pole initially at $E_0+m\hbar\omega$ will move off the real axis, but it could move back onto the real axis, to a point $E_{b'}+m\hbar\omega$ say, as the intensity is turned up still further. This is illustrated in Fig. 2(a). When this happens, the residue of the pole of $f_0(E,\hat{\mathbf{x}})$ at $E=E_{b'}+m\hbar\omega$ must vanish if $m \geq N_0(E_{b'})$ since then $E_{b'}+m\hbar\omega$ is positive (recall the optical theorem). Since $f_m(E_{b'},\hat{\mathbf{x}})$ is proportional to $f_0(E_{b'}+m\hbar\omega,\hat{\mathbf{x}})$, the residue of the pole of $f_m(E,\hat{\mathbf{x}})$ at $E=E_b$ also vanishes if $m \geq N_0(E_{b'})$, and consequently no ionization takes place. This situation is analogous to the vanishing of the photoabsorption cross section at the Fano minimum[20,21] and it gives rise to population trapping.[21,22] If, in the weak-field limit, the resonance pole at $E_r+(m-p)\hbar\omega$ lies directly below the bound-state pole at $E_b+m\hbar\omega$ (a circumstance where the laser frequency is tuned exactly to the Fano minimum, as in Ref. 22) the resonance pole, through its repulsive interaction, actually prevents the bound-state pole from moving off the real axis until the laser intensity is quite strong. A different (perhaps less likely) situation is illustrated in Fig. 2(b). Here it is the (zero-field) resonance pole which moves onto the real axis when the field is turned on. If it moves onto the real axis at the point $E_{r'}+m\hbar\omega$, the residue of the pole of $f_0(E,\hat{\mathbf{x}})$ at $E=E_{r'}+m\hbar\omega$ must vanish for all $m \geq N_0(E_{r'})$. Hence $f_m(E_{r'}-p\hbar\omega,\hat{\mathbf{x}})$ vanishes for all $m \geq N_0(E_{r'}-p\hbar\omega)$. Population trapping can now occur if the electron jumps from the adiabatic eigenvalue curve that develops from E_b onto the adiabatic eigenvalue curve that develops from $E_r-p\hbar\omega$. In Fig. 2(c) we give an example where a bound-state pole moves off and back onto the real axis by passing beneath a threshold. When this happens, $E_{b'}+m\hbar\omega$ is not on the *physical* energy axis if $m \geq N_0(E_{b'})$, and we cannot conclude that the residue of $f_m(E_{b'}-p\hbar\omega,\hat{\mathbf{x}})$ vanishes when $m \geq N_0(E_{b'}-p\hbar\omega)$; pop-

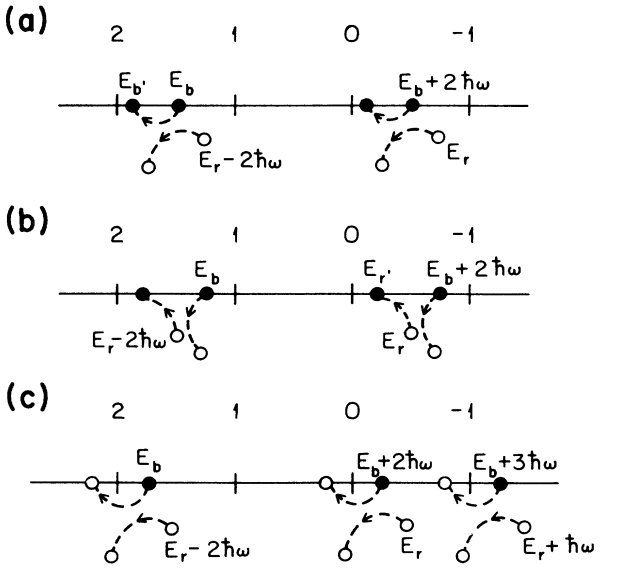

FIG. 2. Some possible pole trajectories for $f_0(E,\hat{\mathbf{x}})$ when there is a bound-state pole close to a resonance pole in the zero-field limit.

ulation trapping cannot occur unless the electron jumps to the adiabatic curve of a shadow pole which also moves onto the physical energy axis.

We have already noted that when a pole moves off the physical energy axis it must move onto an unphysical sheet. (A more rigorous argument, found in many textbooks,[1] goes as follows: A pole on the physical sheet corresponds to an eigenfunction of the Hamiltonian which is normalizable. Therefore the Hamiltonian can be treated as Hermitian. Hence the energy eigenvalue is real, and therefore a pole on the physical sheet must lie on the physical energy axis.) It follows that in Figs. 2(a) and 2(b) the poles on the physical energy axis, at $E_{b'}$ and $E_{r'}$, cannot cross this axis as the intensity is increased further. Rather, these poles must turn back into the lower-half E plane. We therefore expect their trajectories to *osculate* the physical energy axis; hence we expect that a pole situated on this axis remains on this axis through first-order variations of the intensity. This circumstance is obviously favorable to the practical realization of population trapping; the laser intensity need not be sharply defined.

III. SAMPLE CALCULATIONS

In this section we present results of calculations of pole trajectories, versus the field intensity, for a model one-electron system whose atomic potential is

$$W(r)=\beta_1 e^{-\lambda_1 r}/r+\beta_2 e^{-\lambda_2 r}/r \ . \tag{3.1}$$

Within the independent particle approximation, this simulates the atomic potential seen by an electron in a negative ion. We could obtain the Coulomb potential by putting $\lambda_1=\lambda_2=0$, but, as noted earlier, doing this would significantly complicate our discussion since the Coulomb potential supports an infinite number of bound states accumulating at each channel threshold.

To solve the coupled equations (2.6) we expanded the harmonic components $\langle \mathbf{x} \mid \phi_n \rangle$ on a basis set consisting of spherical harmonics, $Y_{lm}(\hat{\mathbf{x}})$, and radial Sturmian functions $S_{nl}^{\kappa}(r)$:

$$S_{nl}^{\kappa}(r)=A_{nl}(-i\kappa r)^{l+1}e^{i\kappa r}\,{}_1F_1(l+1-n,2l+2,-2i\kappa r) \ , \tag{3.2}$$

where κ may be complex and where the normalization factor A_{nl} is independent of κ:

$$A_{nl}=\frac{2^{l+1}}{(2l+1)!}\left[\frac{(n+l)!}{(n-l-1)!}\right]^{1/2} \ . \tag{3.3}$$

Projecting Eqs. (2.6) onto this basis yields a matrix eigenvalue equation; an eigenvalue which is stable with respect to changes in the basis set corresponds to a pole of $f_m(E,\hat{\mathbf{x}})$. We note that rather than use a complex basis set, with $\kappa=|\kappa|e^{i(\pi/2-\theta)}$, we could use a real basis set, with $\kappa=|\kappa|e^{i\pi/2}$, but with the Hamiltonian $H_a+V(t)$ transformed[23,24] by the rotation $r\rightarrow re^{i\theta}$. We prefer to work with the real Hamiltonian and a complex basis set; not only do we find this conceptually more appealing, it is potentially more useful, a point we return to at the end of this section. In all of our calculations we used a basis set consisting of spherical harmonics $Y_{l0}(\hat{\mathbf{x}})$, with $0\le l\le 1$, and Sturmian functions $S_{nl}^{\kappa}(r)$ with $1\le n-l\le 90$.

The Sturmian functions are orthonormal with respect to the weight function $1/r$:

$$\int_0^{\infty} dr(1/r)S_{ml}^{\kappa}(r)S_{nl}^{\kappa}(r)=\delta_{mn} \ . \tag{3.4}$$

This orthonormality condition can be analytically continued to all complex κ. Any well-behaved function of r which vanishes as r^{l+1} for $r\sim 0$ and behaves as $r^{\nu}e^{ikr}$ for $r\sim\infty$ can be expanded in terms of the $S_{nl}^{\kappa}(r)$ with expansion coefficients that vanish for $n\sim\infty$ provided that[25]

$$|\arg(\kappa)-\arg(k)|<\pi/2 \ . \tag{3.5}$$

Note that we require that $0<\arg(\kappa)<\pi$, for otherwise the off-diagonal matrix elements of the Yukawa potential, calculated using the Sturmian basis set, would not, according to (3.5), vanish far off the diagonal.

The boundary condition (2.11a) implies that inequality (3.5) must be satisfied for $k=k_m$, all m, in order for the harmonic components to be expanded on the Sturmian basis set. This certainly cannot be fulfilled on every unphysical energy sheet. To see this, note first that there must exist an integer m_0 for which $\arg(k_{m_0})<0$. [If there did not, we would have $\mathrm{Im}(k_m)>0$, all m, so we would have a pole on the physical energy sheet and the system would not decay.] We are interested only in resonance poles which lie in the lower-half E plane, so that k_{m_0} lies in the lower right quadrant of the k plane, and all other k_m lie either in the lower right or upper left quadrants. We require the angle χ between κ and k_{m_0} in the complex plane to be less than $\pi/2$, according to (3.5). Hence we require κ to lie in the upper right quadrant. (See Fig. 3.)

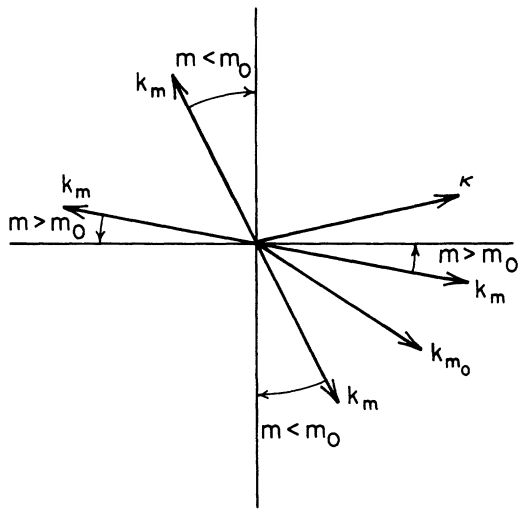

FIG. 3. Orientation of wave numbers in the complex k plane. Note that k_{m_0} lies in the lower right quadrant while k_m lies either in the upper left or lower right quadrant. As m increases (decreases) k_m moves towards the real (imaginary) axis.

If k_m were to lie in the upper left quadrant for $m > m_0$, the angle between k_m and κ would exceed $\pi - \chi$ because k_m moves closer to the real axis as m increases, as illustrated in Fig. 3. Since $\pi - \chi > \pi/2$, inequality (3.5) can be satisfied only if k_m lies in the lower right quadrant for $m > m_0$. For $m < m_0$, k_m may lie either in the upper left or lower right quadrant, subject to one restriction: If there is an m_0' (less than m_0) such that $k_{m_0'}$ lies in the upper left quadrant, k_m must lie in this quadrant for all $m < m_0'$. This follows because the angle χ' between κ and $k_{m_0'}$ must be less than $\pi/2$, and since k_m moves closer to the imaginary axis as m decreases, the angle between κ and k_m would exceed $\pi - \chi' > \pi/2$ for $m < m_0'$ if k_m were to lie in the lower right quadrant. Noting this restriction, we define m_0 so that $m_0 - 1$ is the largest integer for which $\arg(k_m)$ is positive. In summary, our basis set allows us to locate only those poles for which k_m lies in the lower right (upper left) quadrant of the k plane when $m \geq m_0$ ($m < m_0$). These are the poles which can be reached from the physical energy axis by a path which crosses this axis at most once, and therefore these are the poles of greatest physical interest.

We now discuss some results for the case where, in the zero-field limit, $W(r)$ does not support any bound states but does support an s-wave ($l = 0$) shape resonance of energy E_r, where $\mathrm{Re}(E_r) = 7.6715 \times 10^{-3}$ a.u. and $\mathrm{Im}(E_r) = -7.0557 \times 10^{-2}$ a.u. In the zero-field limit $f_0(E, \hat{\mathbf{x}})$ has a resonance pole at $E = E_r$ on the unphysical sheet reached by directly crossing the branch cuts between the thresholds of channels 0 and -1 [on this sheet $\arg(k_m) < 0$ if $m \geq 0$] and it has shadow poles on all other unphysical sheets for which $\arg(k_0) < 0$. We therefore have $m_0 \leq 0$; we cannot locate the shadow poles on those sheets for which $\arg(k_m) > 0$ when $m > 0$. In fact, in this calculation we included only those harmonic components $|\phi_n\rangle$ with channel index in the range $-2 \leq n \leq 2$, and therefore we can only locate the dominant resonance pole ($m_0 = 0$) and two shadow poles ($m_0 = -1$ and -2). The results shown in Fig. 4 would not be significantly altered by the inclusion of more harmonic components, though, of course, we would obtain additional shadow poles. The trajectories of the two shadow poles are seen in Fig. 4 to remain close together; this is a general feature, one that we noticed in studying other resonances (corresponding to different values of the atomic parameters) when there is no interchange of a shadow pole and a dominant one. The shadow poles in Fig. 4 move more swiftly, as the intensity varies, than does the dominant pole, although this is not a general feature. Note that the poles shift to the left as the intensity increases, a general feature noted previously by Ostrovskii.[8] (However, exceptions to this rule occur, for example, when the laser frequency exceeds the smallest dipole-allowed transition frequency.[26]) Thus the real part of the quasienergy becomes increasingly negative. The large shift of the poles to the left is a consequence of removing the spatially independent term in $|\mathbf{A}_0|^2$ from the Hamiltonian, a term whose inclusion would result in a shift to the right of each channel threshold by the ponderomotive energy P. (A significant movement of the trajectory relative to the real axis implies a strong influence of the field on the "width" of the energy and hence on the lifetime of the atomic system.) The shadow poles shown in Fig. 4 shift to the left by very nearly P; in contrast, the dominant pole, whose trajectory moves toward the real axis, shifts by substantially less than P (roughly half). We have not been able to follow the trajectory of the dominant pole at intensities beyond 5×10^{13} W/cm^2, and we do not know whether this pole actually crosses the real axis; however, there is no reason why it could not, since it would cross the real axis to the left of the threshold of channel 0 and would not, therefore, pass onto the physical sheet. It becomes difficult, even impossible, to follow the path of a pole once it passes near to or to the left of the m_0th threshold. This is because k_{m_0} swings through an angle $\sim \pi/2$, becoming almost parallel to the negative imaginary axis in the k plane, and with the restriction that κ lies in the upper right quadrant, Eq. (3.5) cannot be satisfied in practice. (In general, most of the shadow poles that we can in principle observe, can in practice be located only by choosing κ nearly parallel to either the real or imaginary axis, and then their observation is difficult.)

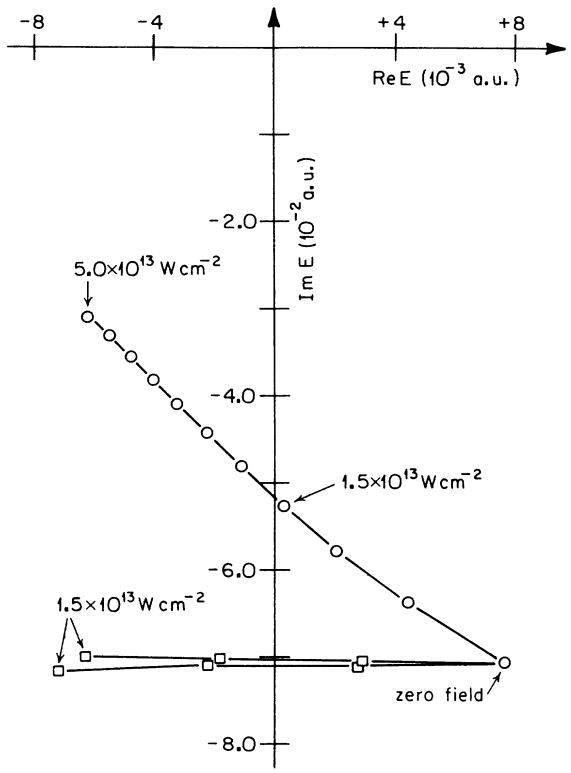

FIG. 4. Trajectories in the complex E plane of an s-wave dominant resonance pole (open circle) and two shadow poles (open squares) of $f_0(E, \hat{\mathbf{x}})$ vs laser intensity. The atomic potential is given by Eq. (3.1) of the text, with parameters (in a.u.) $\beta_1 = -1.85$, $\lambda_1 = 2.0$, $\beta_2 = 0.16$, and $\lambda_2 = 0.30$. The laser light is linearly polarized and of wavelength 532 nm (frequency $\omega \approx 8.5645 \times 10^{-2}$ a.u.). The results shown in Figs. 4, 5, and 8 were calculated at intensity intervals of 0.5×10^{13} W/cm^2; we draw lines through the calculated points to guide the eye.

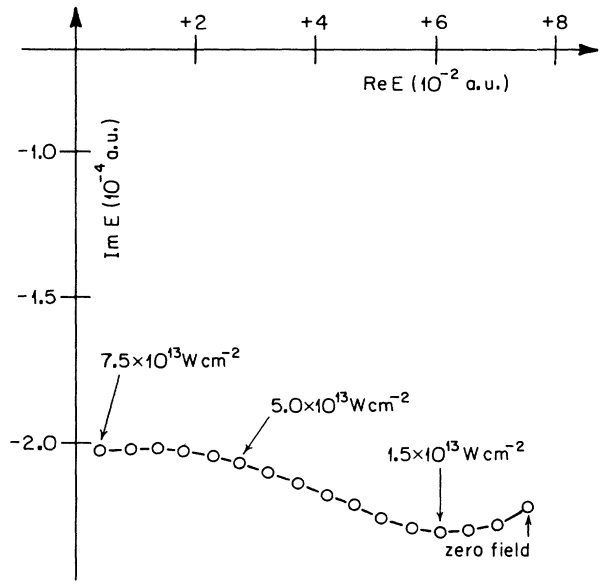

FIG. 5. Trajectory of an s-wave dominant resonance pole of $f_0(E,\hat{\mathbf{x}})$. The atomic potential differs from the potential for Fig. 4 only in that $\beta_1=-6.90$ and $\beta_2=2.70$. We included all harmonic components with channel number in the range $-5\leq n\leq 5$. The light is the same as for Fig. 3.

The movement of a dominant resonance pole of $f_m(E,\hat{\mathbf{x}})$ towards the real axis, as the laser intensity increases, appears to be a general feature when this pole is not far to the right of the threshold of channel m. Another, though less striking, example is shown in Fig. 5. In this example the zero-field width is extremely small, and the pole at first moves away from the real axis when the field is turned on. However, as the intensity is turned up further the pole moves back toward the real axis, a nonperturbative feature. A possible explanation of this behavior is the following: The imaginary part of the energy at the dominant pole is the decay rate, and this is proportional to the available phase space. Now if the coupling of channel m to channels $m'>m$ is negligible, the available phase space is proportional to the square root of $\mathrm{Re}(E-m\hbar\omega)$, with E understood to be the position of the dominant pole. The phase space, and therefore the decay rate,[27] vanish when $\mathrm{Re}(E)<m\hbar\omega$ because the square root becomes imaginary. Therefore, if the coupling of channel m to channels $m'>m$ were truly negligible, and if the dominant pole were to pass to the left of the threshold of channel m, it would actually have to pass through this threshold and then down the real energy axis. Taking into account interchannel coupling, the behavior of the dominant poles shown in Figs. 4 and 5 is not so surprising. In Fig. 5 the dominant pole does not move much closer to the real axis than where it is in the zero-field limit because the width in the zero-field limit is already very small, and coupling to channels $m>0$ prevents the width from shrinking much further. This pole moves to the left by very nearly (slightly less than) the ponderomotive energy P.

This characteristic movement of a dominant resonance pole that is not far to the right of the ionization threshold in the zero-field limit raises an interesting question in regard to the kind of two-color experiment performed by Trainham *et al.*[10] In this experiment Cl^- was neutralized by a relatively weak "ultraviolet" laser in the presence of a strong "infrared" laser, and the photodetachment signal was measured near threshold. Does Cl^- possess a shape resonance just above the ionization threshold? Although there is no evidence that it does, if such a resonance were to exist its width would probably be quite large so that it would not be noticed in ordinary photodetachment by a weak ultraviolet laser. However, a strong infrared laser would shift the resonance down toward the ionization threshold, and possibly below it, and at the same time the width would shrink so that this resonance could play a significant role in the photodetachment process, assuming that it were of the right symmetry and did not shift too far below the threshold.

One does not need to invoke such speculation to shed, perhaps, some light on an interesting puzzle raised by Trainham *et al.*[10] In their experiment they observed that the induced shift in the energy required to neutralize Cl^- was smaller than one might expect from computing the ponderomotive energy of a free electron in the infrared laser. This might be due to the presence of two dominant poles in the neighborhood of the ionization threshold. To see this, consider first the Cl^- ion in the absence of the infrared laser. Suppose that the ultraviolet laser is tuned so that the energy of one high-frequency photon is sufficient, but not by much, to photodetach the electron. Then before the ultraviolet laser is turned on, $f_0(E,\hat{\mathbf{x}})$ has a bound-state pole on the physical energy axis to the right of, and not far from, the threshold of channel 1. This amplitude also has a shadow pole at the same position on the unphysical sheet reached from the bound-state pole via a path which encircles the threshold of channel 1 in a counterclockwise sense. When the ultraviolet laser is turned on these two poles separate, but only very slightly because the intensity of this laser is weak. If, now, the frequency of the ultraviolet laser is reduced, the threshold of channel 1 moves closer to the poles and when it is very close to the poles both of the poles are close to the physical energy axis and are of comparable importance. When the frequency is reduced still further, the threshold moves to the right of the poles, the dominant and shadow poles interchange roles, and photodetachment can no longer occur via the absorption of one photon. Note, however, that the shadow pole which becomes the dominant pole as the threshold is passed is not significant because when it becomes the dominant pole its contribution is of second-order in smallness in the sense that it contributes to the weak *two*-photon detachment signal. Suppose now that instead of reducing the original frequency of the ultraviolet laser we turn on the infrared laser. As we increase the intensity of the powerful infrared laser the poles move to the left towards the threshold of channel 1, and they begin to separate significantly. Now the *two poles simultaneously contribute significantly* to the photodetachment signal; the shadow pole which crosses the threshold contributes to the nonnegligible *two*-photon *two*-color signal. (Note that the ponderomotive energy is of the same order as the average energy ab-

sorbed by an electron in the continuum.[28]) This suggests that the analysis based on the trajectory of a single pole should be reconsidered.

We now address the question of how we can tell whether an energy eigenvalue, which is stable with respect to enlarging the basis set, corresponds to a dominant pole or a shadow pole. Stated another way, how do we know which sheet the energy eigenvalue is on? The answer is provided by considering the allowed orientation of κ. Suppose we find an eigenvalue E which lies below the real energy axis between the thresholds of channels l_0 and l_0-1. If this eigenvalue corresponds to a dominant pole it can be directly reached from the physical energy axis along a downward vertical path commencing on this axis between the thresholds of channels l_0 and l_0-1. In this case, k_m lies in the lower right quadrant if $m \geq l_0$ and in the upper left quadrant if $m < l_0$. This now determines the allowed range of orientations of κ: We can choose all κ for which Eq. (3.5) is satisfied with $k = k_{l_0}$ and $k = k_{l_0-1}$ [subject to $\arg(x) > 0$]. If the eigenvalue E really does correspond to a dominant pole, it must remain stable as the orientation of κ is varied throughout this range. If stability is not observed in this range, E cannot correspond to a dominant pole; it must correspond to a shadow pole. In this case, there is an integer m_0 such that k_m lies in the lower right quadrant if $m \geq m_0$ and in the upper left quadrant if $m < m_0$. The allowed range of orientations of κ is given by Eq. (3.5) with $k = k_{m_0}$ and $k = k_{m_0-1}$. We choose various values of m_0 until we observe the predicted stability for the particular m_0; this tells us on which sheet the shadow pole lies. In Fig. 6 we show the stability regions, at a fixed laser intensity, for the dominant pole and two shadow poles shown in Fig. 4. In Fig. 7 we show the stability regions for three shadow poles arising from a different s-wave resonance in the zero-field limit. The stability regions overlap, and in principle we ought to be able to see two poles in the overlap region. In practice it is difficult to see more than one pole in the overlap region because there are numerical instabilities in this region. Furthermore, the boundaries of the various stability regions are not always respected in our calculations; we often find the range of stability to be either slightly wider or narrower than predicted. This is presumably due to minor inaccuracies of the calculation stemming from the inclusion of an insufficient number of both spherical harmonics and harmonic components; one consequence is that the asymptotic boundary condition (2.11a) is not satisfied, and this in turn affects our analysis of the stability regions.

It is particularly difficult to follow the path of a resonance pole which starts as a bound-state since it does not usually move far below the real axis before it reaches the first threshold, and so when it does pass this threshold k_{m_0} swings very rapidly (through $\sim\pi/2$). In Fig. 8 we show the trajectory of a resonance pole, which starts as a

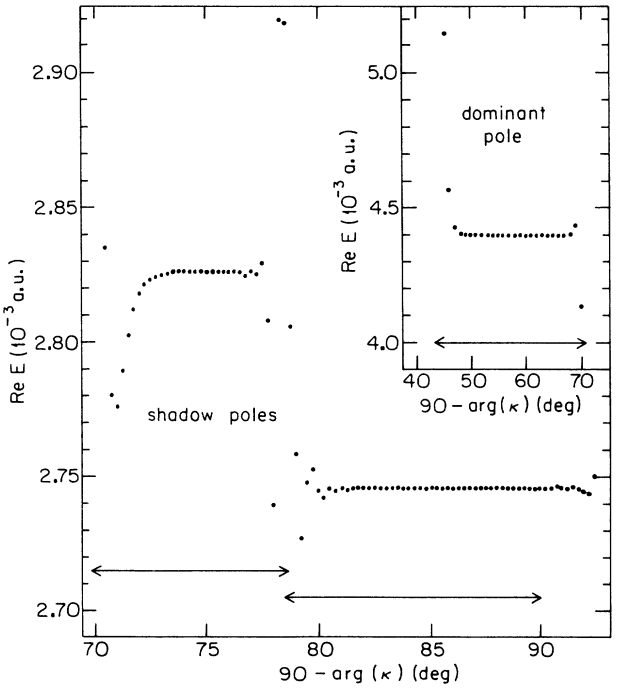

FIG. 6. Stability regions for the poles shown in Fig. 4 at the intensity 5×10^{12} W/cm^2. The vertical axis is the real part of the energy. The horizontal axis measures the orientation of κ relative to the positive imaginary axis. The predicted range of stability is indicated by $\leftrightarrow$. In Figs. 6, 7, and 9 we show raw data obtained from the solution of the matrix eigenvalue equation discussed in the text.

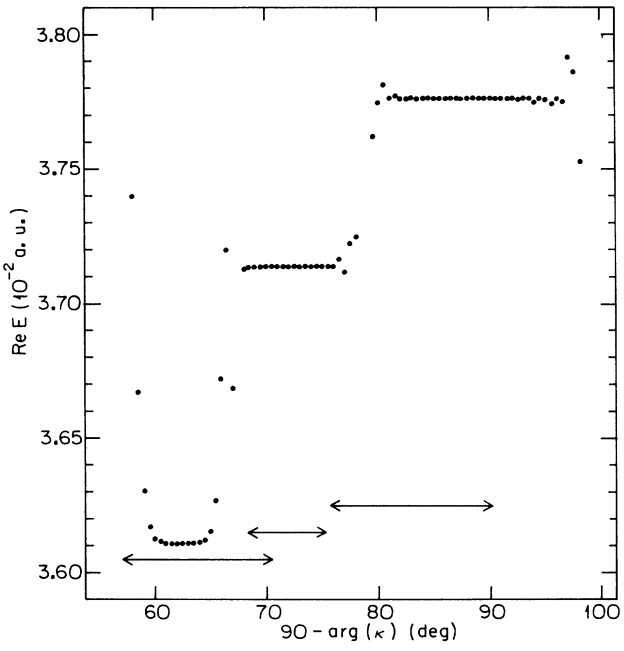

FIG. 7. Stability regions at a fixed intensity for three shadow poles born from a resonance pole which is at $E_r = 0.00791 - 0.123i$ in the zero-field limit. The atomic parameters are (in a.u.) $\beta_1 = -2.25$, $\lambda_1 = 2.0$, $\beta_2 = 0.36$, and $\lambda_2 = 0.30$. We included all harmonic components with channel number in the range $-3 \leq n \leq 3$. The laser light is linearly polarized, with wavelength 532 nm and intensity 4×10^{13} W/cm^2.

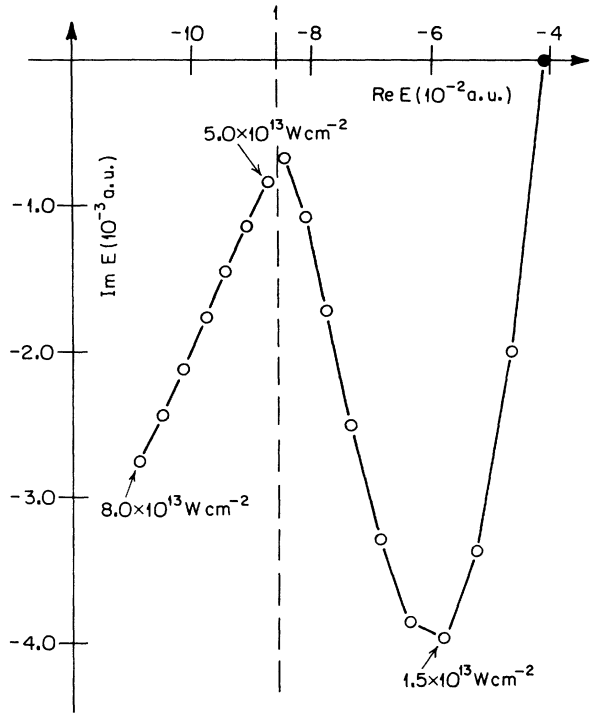

FIG. 8. "Diabatic" trajectory of the dominant resonance pole which is born from a bound-state pole. The resonance pole which is the dominant pole to the right of the threshold of channel 1 interchanges roles with a nearby shadow pole when it crosses to the left of this threshold. The atomic parameters are $\beta_1=-2.0$, $\lambda_1=2.0$, and $\beta_2=0$. We included all harmonic components with channel number in the range $-3\leq n\leq 3$. The laser light is linearly polarized and of wavelength 532 nm (frequency $\omega=8.5645\times10^{-2}$ a.u.).

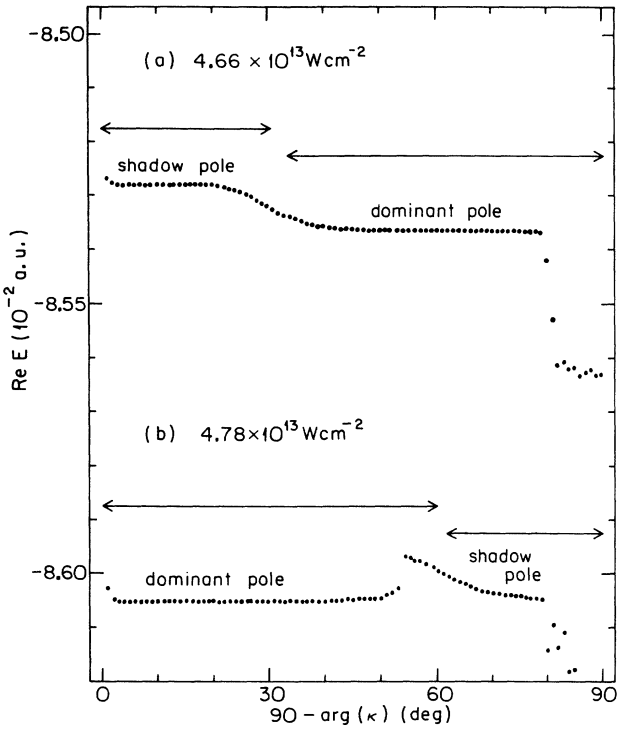

FIG. 9. Stability regions, at two different intensities, for the dominant pole shown in Fig. 8, and the nearby shadow pole. The two intensities are both very close to the intensity at which the dominant pole crosses the threshold. In this intensity region we are able to locate both the dominant pole and the nearby shadow pole. (a) Intensity is slightly below the intensity at which the threshold is passed. (b) Intensity is slightly above the threshold intensity. In (a) the imaginary parts of the eigenvalues (not shown) are similar for the shadow and dominant poles, while in (b) the imaginary parts differ by about 15%.

bound-state pole, up to the point where it reaches the first threshold. We cannot follow this pole at higher intensities ($\gtrsim 5\times10^{13}$ W/cm^2); it changes roles with a shadow pole. The trajectory shown to the left of the threshold is that of the dominant pole. Note that the diabatic curve exhibits a sharp bend at the threshold, where it passes from one unphysical sheet to another. The sharp bend in the adiabatic trajectory to the right of the threshold is a consequence of the reduction in available phase space as the threshold is approached; this was discussed above. Stability regions at the two intensities close to the intensity where the threshold is crossed are shown in Fig. 9.

We end this article by briefly commenting on the inadequacy of our basis. It should now be apparent that the chief inadequacy is the failure to satisfy inequality (3.5) for k equal to all possible k_m. This is a consequence of choosing only one wave number κ for the Sturmian basis functions. However, we could alleviate this difficulty by introducing two types of Sturmian basis functions, $S_{nl}^{\kappa_i}(r)$, $i=1,2$, where κ_i lies in the upper left ($i=1$) or lower right ($i=2$) quadrant of the k plane. (The method of complex coordinates does not appear to have a similar extension since we cannot introduce two different rotated Hamiltonians.) It might seem that such as basis would be overcomplete; this is not so because the spaces spanned by the $S_{nl}^{\kappa_i}(r)$ are not equivalent for different i. For example, we can expand $r\exp(-\mu r)$ in terms of the $S_{n0}^{\kappa_i}(r)$; were we to take κ_1 and κ_2 along the positive and negative imaginary axes, respectively, the coefficients of the Sturmian functions whose wave number is κ_2 would simply vanish. Unfortunately, there is no orthogonality relation between Sturmian functions with different wave number, and this significantly complicates the calculation. Nevertheless, this is the path we shall explore in future calculations.

ACKNOWLEDGMENTS

This work was supported by the National Foundation under Grant No. PHY-87-13196. We are grateful for computer time at the San Diego Supercomputer Center.

APPENDIX: EXPRESSION FOR THE ABSORPTION AMPLITUDE

The differential rate, denoted as $dR_N/d\Omega$, for electrons to absorb $N\geq N_0$ photons and emerge with mean speed $v_N=\hbar k_N/\mu$ into the solid angle $d\Omega$ along the direction $\hat{\mathbf{k}}_N$ is, with $|\Phi(t)\rangle$ properly normalized,

$$dR_N/d\Omega = v_N |f_N(E,\hat{\mathbf{k}}_N)|^2 . \quad \text{(A1)}$$

Here N_0 is the smallest integer n for which $E+n\hbar\omega>0$. If the electrons are incident from infinity, we take E to be the incident free-particle energy. If, on the other hand, the electrons are initially bound, we take E to be the *real* energy that is closest to the complex energy E_p of the dominant pole which develops from the zero-field bound-state pole of $f_0(E,\hat{\mathbf{x}})$. The reason we must neglect the width Γ of E_p in the evaluation of the rate is that the rate is a physical quantity, and therefore real; were we to retain Γ, the speed v_N would be complex on the right-hand side of Eq. (A1). Moreover, if Γ were kept we would have $\mathrm{Im}(k_m)<0$ for $m\geq N_0$ and, referring to the asymptotic form (2.11a), the terms $m\geq N_0$ of each harmonic component would explode exponentially for $r\rightarrow\infty$, as $\exp(\Gamma r/2\hbar v_m)$ if we assume that

$$\Gamma \ll \mathrm{Re}(E_p)+N_0\hbar\omega . \quad \text{(A2)}$$

This last inequality is, in fact, just the condition under which Γ can be neglected since the significant range or r in the mth channel is of the order of the de Broglie wavelength $1/k_m$, and $\exp(\Gamma r/2\hbar v_m)$ is unity over this range if (A2) is satisfied.

We now utilize Eqs. (2.11) to derive two different expressions for the N-photon absorption amplitude, $f_N(E,\hat{\mathbf{x}})$, for $N\neq 0$. We start by assuming that the atomic potential W does not have a Coulomb tail. The first expression is in terms of matrix elements of the coupling $V_\pm$ of the electron with the field; it remains valid if, at the end, we let W acquire a Coulomb tail. The other expression is in term of matrix elements of W, and is valid only if $rW\sim 0$ for $r\sim\infty$. We introduce the matrix element

$$M_{Nn}\equiv\langle\Phi^-_{\mathbf{k}_N}|(H_a^\dagger-H_a)|\phi_n\rangle , \quad \text{(A3)}$$

where $|\Phi^-_{\mathbf{k}}\rangle$ represents an electron which elastically scatters from W in the absence of radiation and emerges with momentum $\hbar\mathbf{k}$. Note that $\langle\Phi^-_{\mathbf{k}}|\Phi^-_{\mathbf{k}'}\rangle = a_k^2\delta^3(\mathbf{k}-\mathbf{k}')$, where the density of states in a narrow energy interval is $(\mu k/\hbar^2 a_k^2)d\hat{\mathbf{k}}$. Using Green's theorem we can transform the volume integral of Eq. (A3) into an integral over a surface of very large radius, and we can evaluate this surface integral by using the asymptotic forms of $\langle\mathbf{x}|\phi_n\rangle$ and $\langle\mathbf{x}|\Phi^-_{\mathbf{k}}\rangle$. The asymptotic form of $\langle\mathbf{x}|\Phi^-_{\mathbf{k}}\rangle$ consists of the plane wave $a_k\langle\mathbf{x}|\mathbf{k}\rangle$ where $\langle\mathbf{x}|\mathbf{k}\rangle=(2\pi)^{-3/2}\exp(i\mathbf{k}\cdot\mathbf{x})$, plus an *in*going scattered wave. This ingoing scattered wave becomes *out*going upon complex conjugation, and the product of this and $\langle\mathbf{x}|\phi_n\rangle$ yields a contribution to the surface integral which oscillates as r varies, since $\langle\mathbf{x}|\phi_n\rangle$ is a plane wave with amplitude C_n and wave number k_0 ($\neq k_N$ since $N\neq 0$) plus a superposition of *out*going waves. In fact, the only contribution to the surface integral which does not oscillate comes from the product of $\langle\mathbf{x}|\mathbf{k}_N\rangle^*$ and the Nth term of $\langle\mathbf{x}|\phi_n\rangle$, that is, the term in $f_{Nn}(E,\hat{\mathbf{x}})$. Neglecting the oscillatory contributions, which average to zero over a macroscopically small volume (provided E is real), we find, after a little manipulation, that

$$M_{Nn}=-(2\pi)^{-3/2}(2\pi\hbar^2 a_{k_N}/\mu)f_{Nn}(E,\hat{\mathbf{k}}_N) . \quad \text{(A4)}$$

Putting $n=N$, and using Eq. (2.11c), it follows that

$$f_N(E,\hat{\mathbf{k}}_N)=-(2\pi)^{3/2}(\mu/2\pi\hbar^2 a_{k_N})M_{NN}/J_0(\rho_N) . \quad \text{(A5)}$$

If we let $H_a^\dagger$ act on the bra in Eq. (A3), noting that $H_a|\Phi^-_{\mathbf{k}}\rangle=(\hbar^2k^2/2\mu)|\Phi^-_{\mathbf{k}}\rangle$, we obtain, on putting $n=N$ and using Eqs. (2.6) and (2.9),

$$M_{NN}=\langle\Phi^-_{\mathbf{k}_N}|V_-|\phi_{N+1}\rangle+\langle\Phi^-_{\mathbf{k}_N}|V_+|\phi_{N-1}\rangle \quad \text{(A6)}$$

Equations (A5) and (A6) express the N-photon absorption amplitude in terms of matrix elements of $V_\pm$; the expression remains valid if we now let W acquire a Coulomb tail. We can derive an alternative expression by first considering

$$M_N\equiv\sum_n e^{i(N-n)\chi_N}J_{n-N}(\rho_N)M_{Nn} \quad \text{(A7a)}$$

$$=-(2\pi)^{-3/2}(2\pi\hbar^2 a_{k_N}/\mu)f_N(E,\hat{\boldsymbol{\kappa}}_N) , \quad \text{(A7b)}$$

where in the second step we used Eqs. (A4) and (2.11c) to express M_{Nn} in terms of $f_N(E,\hat{\boldsymbol{\kappa}}_N)$, and we observed that the sum of $J_n(z)^2$ over all n is unity. We now use Eqs. (2.5) and (A3), and the integral representation of the Bessel function, to reexpress Eq. (A7a) as

$$M_N=\frac{\omega}{2\pi}\int_0^{2\pi/\omega}dt\, e^{i\mathbf{k}_N\cdot\boldsymbol{\alpha}(t)+iN\omega t}\times\langle\Phi^-_{\mathbf{k}_N}|(H_a^\dagger-H_a)|\Phi(t)\rangle . \quad \text{(A8)}$$

We replace the bra in the matrix element on the right-hand side of Eq. (A8) by $a_{k_N}\langle\mathbf{k}_N|$, since (as before) the scattered wave in $\langle\Phi^-_{\mathbf{k}_N}|$ does not contribute to the nonoscillatory part of the surface integral. Noting that

$$[(\mathbf{p}^2/2\mu)+V(t)-i\hbar\,d/dt]\times e^{-i\mathbf{k}_N\cdot\boldsymbol{\alpha}(t)-i(E+N\hbar\omega)t/\hbar}|\mathbf{k}_N\rangle=0 , \quad \text{(A9)}$$

and using Eq. (2.3), we obtain

$$M_N=(\omega/2\pi)a_{k_N}\int_0^{2\pi/\omega}dt\, e^{if(t)}\langle\mathbf{k}_N|\times[W-V(t)-H_a-i\hbar(d/dt)^\dagger]\times|\Psi(t)\rangle ,$$

where $f(t)=\mathbf{k}_N\cdot\boldsymbol{\alpha}(t)+N\omega t+Et/\hbar$, and where the adjoint of the time derivative implies this derivative acts to the left. Integrating by parts over t, noting that the surface term vanishes because the integrand is periodic, and using Eq. (2.4), we arrive at

$$M_N=(\omega/2\pi)a_{k_N}\int_0^{2\pi/\omega}dt\, e^{iN\omega t+i\mathbf{k}_N\cdot\boldsymbol{\alpha}(t)}\langle\mathbf{k}_N|W|\Phi(t)\rangle$$

$$=a_{k_N}\sum_n e^{i(N-n)\chi}J_{n-N}(\rho_N)\langle\mathbf{k}_N|W|\phi_n\rangle . \quad \text{(A10)}$$

Combining Eqs. (A7b) and (A10) we have an expression for the N-photon absorption amplitude in terms of matrix elements of W (but we cannot let W acquire a Coulomb tail).

The expression for $f_N(E,\hat{\mathbf{x}})$ obtained by combining Eqs. (A5) and (A.6) is, as far as we know, new. We recently used it[29] to calculate rates for multiphoton ionization of H. The expression obtained by combining Eq. (A7b) and (A10) was derived earlier in a different way,[12] and was used to calculate rates for multiphoton detachment of H^-.

[1]See, e.g., J. R. Taylor, *Scattering Theory* (Wiley, New York, 1972).

[2]R. J. Eden and J. R. Taylor, Phys. Rev. **133B**, 1575 (1964).

[3]For a list of early references see C. E. Jones, Ann. Phys. **31**, 481 (1965).

[4]D. Morgan, Phys. Lett. **51B**, 71 (1975); Y. Fujii and M. Fukugita, Nucl. Phys. B **85**, 179 (1975).

[5]R. E. Brown, N. Jarmie, and G. M. Hale, Phys. Rev. C **35**, 1999 (1987).

[6]A. Herzenberg and D. Ton-That, J. Phys. B **8**, 426 (1975).

[7]P. G. Burke, J. Phys. B **1**, 586 (1968). See also C. J. Chapman and A. Herzenberg, *ibid.* **5**, 790 (1972); M. Ohno and W. Domcke, Phys. Rev. A **28**, 3315 (1983).

[8]V. N. Ostrovskii, Teor. Mat. Fiz. **33**, 126 (1977) [Theor. Math. Phys. **33**, 923 (1977)]. See also V. N. Ostrovsky and D. A. Telnov, J. Phys. B **20**, 2397, (1987); **20**, 2421 (1987).

[9]See, e.g., T. J. McIlrath, P. H. Bucskbaum, R. R. Freeman, and M. Bashkansky, Phys. Rev. A **35**, 4611 (1987).

[10]R. Trainham, G. D. Fletcher, N. B. Mansour, and D. J. Larson, Phys. Rev. Lett. **59**, 2291 (1987).

[11]See, e.g., J. H. Shirley, Phys. Rev. **138**, B979 (1965); N. M. Kroll and K. M. Watson, Phys. Rev. A **8**, 804 (1973). For a review of Floquet methods, applied to ionization processes, see S.-I. Chu, Adv. At. Mol. Phys. **21**, 197 (1985).

[12]R. Shakeshaft and X. Tang, Phys. Rev. A **36**, 3193 (1987).

[13]For a rigorous mathematical discussion of the connection between the poles of the scattering amplitude and the complex eigenvalues of the Schrödinger equation for an atom interacting with a monochromatic radiation field, see S. Graffi, V. Grecchi, and H. J. Silverstone, Ann. Inst. Henri Poincaré **42**, 215 (1985) and references therein.

[14]R. Shakeshaft, Z. Phys. D **8**, 47 (1988); M. Edwards and R. Shakeshaft, *ibid.* **8**, 51 (1988); R. Potvliege and R. Shakeshaft, Phys. Rev. A **38**, 4597 (1988).

[15]The Floquet ansatz gives an exact description of a scattering process because the initial state of the electron, that of a free particle, is insensitive to switching on the field. On the other hand, in an ionization process the initial state is a bound state, and it is sensitive to switching on the field—the moment the field is switched on the atom begins to disintegrate—and so the Floquet ansatz gives only an approximate description.

[16]H. H. Muller, A. Tip, and M. J. van der Wiel, J. Phys. B **16**, L679 (1983).

[17]R. Potvliege and R. Shakeshaft, Phys. Rev. A **38**, 4597 (1988).

[18]We assume none of the poles cross the real energy axis. If a shadow pole of $f_m(E,\hat{\mathbf{x}})$, born from a resonance pole of this amplitude, were to cross the real axis to the right of the threshold of channel m and subsequently cross the real axis again, an odd number of times, to the left of this threshold, it could move close to (and below) the physical energy axis. We regard this as an interesting but exceptional case.

[19]R. Bhatt, B. Piraux, and K. Burnett, Phys. Rev. A **37**, 98 (1988).

[20]U. Fano, Phys. Rev. **124**, 1866 (1965).

[21]P. T. Greenland, J. Phys. B **15**, 3191 (1982).

[22]See, e.g., P. Lambropoulos and P. Zoller, Phys. Rev. A **24**, 379 (1981); P. E. Coleman and P. L. Knight, J. Phys. B **15**, L235 (1982).

[23]For reviews of complex scaling methods see B. R. Junker, Adv. At. Mol. Phys. **18**, 207 (1982); W. P. Reinhardt, Ann. Rev. Phys. Chem. **33**, 223 (1982).

[24]Calculations of resonance eigenvalues based on using the rotated Hamiltonian for an atom in a field have been performed by, e.g., S.-I. Chu and J. Cooper, Phys. Rev. A **32**, 2769 (1985) for hydrogen and by Th. Mercouris and C. A. Nicolaides, J. Phys. B **21**, L285 (1988) for H^-.

[25]R. Shakeshaft, Phys. Rev. A **34**, 244 (1986); **34**, 5119 (1986).

[26]Another exception, discussed by Ostrovskii (Ref. 8), occurs if there is an "antibound" (virtual) state pole in the zero-field limit; such a pole sits on the real energy axis but on an unphysical sheet. If $f_m(E,\hat{\mathbf{x}})$ has an antibound pole in the zero-field limit it sits to the left of the threshold of channel m, and when the field is turned on it is likely to at first move to the right, around the threshold of channel m, and onto a new unphysical sheet on which it subsequently moves to the left, closer to the physical energy axis.

[27]The decay rate does not vanish when the atomic potential has a Coulomb tail because the ionization matrix element is singular at the threshold.

[28]R. Shakeshaft, J. Opt. Soc. Am. B **4**, 705 (1987). See pp. 717–718.

[29]R. M. Potvliege and R. Shakeshaft, Phys. Rev. A **38**, 1098 (1988).